

Kinetic model for the catalytic disproportionation of pine oleoresin over Pd/C catalyst



Linlin Wang, Xiaopeng Chen*, Wenjing Sun, Jiezhen Liang, Xu Xu, Zhangfa Tong

School of Chemistry and Chemical Engineering, Guangxi University, Key Laboratory for the Petrochemical Resources Processing and Process Intensification Technology of Guangxi, Nanning 530004, PR China

ARTICLE INFO

Article history:

Received 19 November 2012

Received in revised form 4 April 2013

Accepted 7 April 2013

Keywords:

Pine oleoresin

Disproportionation

Kinetic model

Carbon-supported palladium catalyst

ABSTRACT

The kinetics of the disproportionation of pine oleoresin (a renewable bioresource) over a carbon-supported palladium catalyst was studied. Kinetic experiments, constructed to eliminate internal and external mass transfer limitations, were performed in the temperature range of 210–250 °C. The samples, withdrawn from reaction mixtures at different intervals, were determined by GC–MS and GC. A new reaction scheme together with a lumped kinetic model was proposed to describe the complex reaction system. The kinetic parameters for each involved reaction were estimated using the Levenberg–Marquart method by MATLAB software. The various activation energies of rosin acids in pine oleoresin, for the isomerization, dehydrogenation and hydrogenation reactions, were 83.05–172.75 kJ mol^{−1}. The various activation energies of monoterpenes in pine oleoresin, for the dehydrogenation and hydrogenation reactions, were 103.97–133.82 kJ mol^{−1}. The kinetic model well fitted the experimental observations and could be used to predict the concentration distribution of the products at 260 °C. The results showed that the disproportionations of rosin acids and monoterpenes followed second order and first order reactions, respectively. In addition, dehydrogenation was the main reaction in the disproportionation of pine oleoresin. Dehydrogenated acid and *p*-cymene were main components in the final products.

© 2013 The Authors. Published by Elsevier B.V. Open access under [CC BY-NC-ND license](http://creativecommons.org/licenses/by-nc-nd/4.0/).

1. Introduction

With the gradual decrease of the fossil resources, there is an ever-increasing interest for the use of renewable resources in making more valuable products (Piang-Siong et al., 2012). Pine oleoresin is an important forestry product, traditionally obtained by tapping the bark of living pine tree and collecting the resultant exudates (Rezzi et al., 2005). Rosin and turpentine are the major products from pine oleoresin by steam distillation. Rosin is composed mostly of rosin acids and some neutral matter. Approximately 90% of the rosin acids are the abietic-type resin acids with conjugated double bonds and a single carboxylic group. The other 10% are the closely related pimaric-type resin acids with non-conjugated double bonds (Enos et al., 1968). Both of them have a typical formula C₁₉H₂₉COOH. The principal components of turpentine are bicyclic monoterpenes, such as α -pinene, β -pinene and carene, with a general formula C₁₀H₁₆ (Rezzi et al., 2005; Song et al., 1995).

Rosin can be modified to “disproportionated rosin” via a catalytic disproportionation reaction since the abietic-type resin acids contain chemically reactive conjugated double bonds. Because of its advantages (i.e., low brittleness, high thermal stability, good oxidation resistance to light color), the disproportionated rosin (dehydroabietic acid plus a small amount of hydrogenation resin acids) is widely used in the production of butadiene and chloroprene rubber, ABS resin, adhesives, solder flux, printing inks and paper of neutral-size (Mayer et al., 1996; Soltes and Zinkel, 1989; Souto et al., 2011). Dehydroabietic acid, a main component of disproportionated rosin, possesses aromatic diterpene structure that having three benzene rings, three chiral carbon atoms, and a reactive carboxy group. It can be used as a starting material for the synthesis of many important multifunctional derivatives (Wang et al., 2010). A number of its derivatives have many biological activities, such as anti-cancer, analgesic, spasmolytic, anti-inflammatory and insecticidal effects (Häkkinen et al., 2012; Souto et al., 2011). Therefore, they become the interest additives in the development of new drugs or fine chemicals, such as antimicrobial, antitumor, antioxidant, gastroprotective, K⁺ channel-opening activities and chiral surfactants (Gu and Wang, 2010; Rajakumar et al., 2009; Thevisen et al., 2009; Wang et al., 2010).

Due to the presence of a double bond and a strained four-membered ring, pinene readily undergoes various transformations. A refined route to *p*-cymene can start from the transformation of

* Corresponding author. Tel.: +86 771 3272702; fax: +86 771 3233718.

E-mail address: lilm@gxu.edu.cn (X. Chen).

Notation

A	bicyclic monoterpenes
B	palustric acid
C	neoabietic acid
<i>c</i>	concentration of compound, mol L ⁻¹
\hat{c}	calculated concentration of component, mol L ⁻¹
D	pimaric-type resin acids
<i>d</i>	density of product liquid, g cm ⁻³
E	hydrogenated monoterpenes
<i>E_a</i>	activation energy, kJ mol ⁻¹
F	monocyclic monoterpenes
<i>F_t</i>	tabled values of <i>F</i> -test
G	abietic acid
<i>G_d</i>	mass of disproportionated product, g
H	hydrogenated pimarenoic-type resin acids
I	<i>p</i> -cymene
J	dehydroabietic acid
K	hydrogenated abietic-type resin acids
<i>k</i>	rate constant for reaction, min ⁻¹ , L mol ⁻¹ min ⁻¹
<i>k₀</i>	frequency factor, min ⁻¹ , L mol ⁻¹ min ⁻¹
<i>M</i>	molecular weight, g mol ⁻¹
<i>Q</i>	sum of square of residuals, target function value
<i>r</i>	reaction rate, mol min ⁻¹ L ⁻¹
<i>t</i>	time, min
<i>W</i>	mass of product liquid, g

Greek letters

ρ^2	correlation coefficient of model
ω	mass fraction, %

Subscript

<i>i</i>	<i>i</i> th component in the mixture
----------	--------------------------------------

monoterpenes containing a similar structure (Al-Wadaani et al., 2009; Buhl et al., 1998; Martín-Luengo et al., 2008; Roberge et al., 2001). *p*-Cymene is an important product and valuable intermediate in the chemical industry. It is used in the fragrance industry and as an important starting material for the production of intermediates like *p*-cresol. And it is also a raw material for the synthesis of non-nitrated musks, which nowadays tends to replace nitrated ones (Al-Wadaani et al., 2009; Buhl et al., 1998; Martín-Luengo et al., 2008; Roberge et al., 2001; Zhang et al., 2010).

Generally, the disproportionated rosin and *p*-cymene can be produced from rosin (Song and Liang, 1997; Song et al., 1985) and turpentine over different catalysts (Al-Wadaani et al., 2009; Buhl et al., 1998; Martín-Luengo et al., 2008; Roberge et al., 2001), respectively. However, they must be steam-distilled from crude oleoresin at first. Such a long process implies high cost on energy consumption. Conventional preparation of *p*-cymene is also based on the Friedel–Crafts alkylation of petroleum derivatives: benzene with methyl and isopropyl halides using AlCl₃ as an acid catalyst, or toluene with isopropyl alcohol. Moreover, using highly toxic substances such as benzene or toluene and AlCl₃ is more restricted by environmental legislation in industrialised countries (Martín-Luengo et al., 2008). Abundant pine oleoresin resources are available in China. And its production is more than 500 kt a⁻¹, taking it the first place in the world (Song, 2004). Since oleoresin is a low cost, low toxicity forest biomass resource available in China, attentions are paid to the production of modified with increased added-value materials. Thus, the conversion of renewable oleoresin to the disproportionated rosin and *p*-cymene is of high commercial interest. We found that pine oleoresin could be transformed to the disproportionated rosin and

p-cymene over a Pd/C catalyst (Chen et al., 2004; Wang et al., 2007a) (see Scheme 1), and the contents of dehydroabietic acid (based on disproportionation rosin) and *p*-cymene (based on disproportionation turpentine) in the disproportionation products were 60–75% and 40–60%, respectively. More details can be found in our patent (Chen et al., 2004) and publications (Wang et al., 2007a,b). Moreover, the viscosity of reaction system was reduced so that the liquid–solid mass transfer was improved by the turpentine solvent contained in the oleoresin itself. As a result, the dehydro-aromatization of the abietic acid was strengthened. Several studies concerning the reaction process for the preparation of the disproportionated rosin from rosin (Loeblich and Lawrence, 1956; Song and Liang, 1997; Song et al., 1985) and the *p*-cymene from monoterpenes (Al-Wadaani et al., 2009; Buhl et al., 1998; Martín-Luengo et al., 2008, 2010; Roberge et al., 2001) have been published. There are two kinds of main reactions, i.e., isomerization and disproportionation, involved in the preparations of disproportionated rosin and *p*-cymene. However, no specific reports have been published about the reaction kinetics for the catalytic isomerization and disproportionation of oleoresin over a Pd/C catalyst.

The present paper focused on the reaction kinetics. First, the external and internal diffusion resistances were investigated. Second, the kinetic experiments were performed in the temperature range 210–260 °C under the kinetic control regime. Third, the reaction mixtures, successfully used in the complex kinetics of petroleum refining processing (Bollas et al., 2007; Hernández-Barajas et al., 2009; Lin et al., 2001; Meng et al., 2006; Singh et al., 2005; Zhou et al., 2008), were divided into 7 lumps in light of the lumping method. Finally, based on the reaction characteristics and the experimental results, the kinetic model was proposed. And the various parameters (rate constants and activation energies) were estimated by the Levenberg–Marquart method with MATLAB programming.

2. Experimental

2.1. Material and catalyst

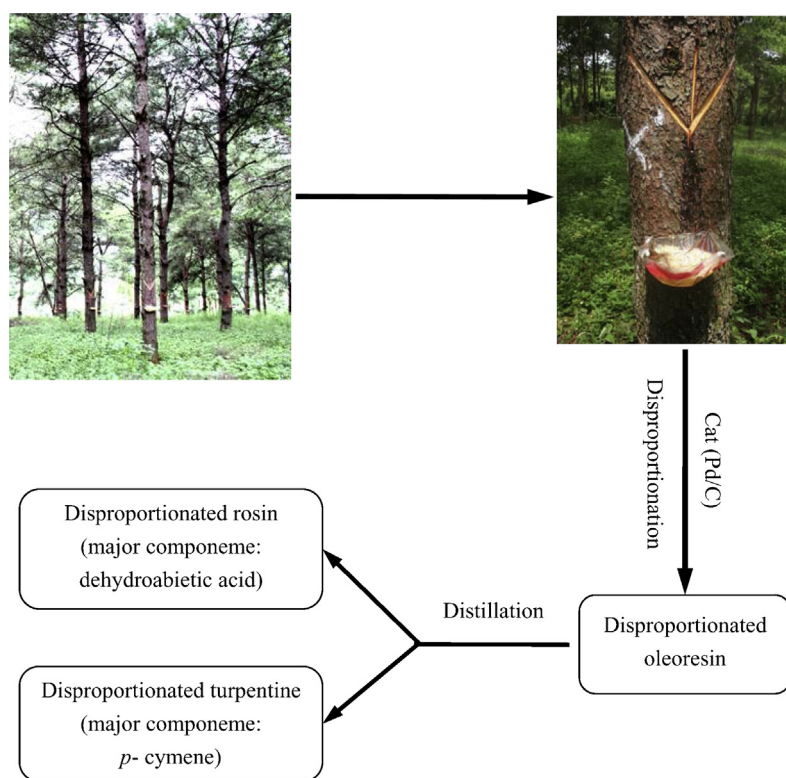
The starting reactant, pine oleoresin of *P. massoniana* was purchased from Guangxi Wuzhou Pine Chemicals Ltd., China.

The Pd/C catalyst was prepared from palladium chloride (Shanghai Xingao Chemical Reagent Co. Ltd., China; palladium content by weight ≥59%) by the conventional method described in the publications (Tike and Mahajani, 2006) and (Drelinkiewicz and Waksmundzka-Góra, 2006).

The specific surface area (BET), total pore volume and average pore diameter were measured in duplicate by nitrogen adsorption at –196 °C in a Quantachrome NOVA 1200 instrument. The mean particle size distribution of the catalyst was measured with a Malvern Mastersizer. The SEM–Energy-Dispersive X-ray System (EDS) analysis on an S-3400 N Scanning Electron Microscopy gave an idea of the distribution of Pd on carbon particles, using an acceleration voltage of 25 kV. Basic characteristics of the Pd/C catalyst were obtained as follows: BET specific surface area was 927.4 m² g⁻¹, the metal loading 4.68 wt%, mean particle size 16 μm, total pore volume 0.56 cm³ g⁻¹, average pore diameter 13.5 Å.

2.2. Experimental procedure and sample analysis

The reaction runs were performed in a 2 L stainless steel stirred batch reactor (Dalian Tongchan Autoclave Vessel Manufacturing Co. Ltd., China) equipped with an internal thermocouple, a pressure transducer (Matsushita Electric Works Ltd., Japan), a cooling coil



Scheme 1.

with a circulating cold water, and a sampling valve. A double-tier paddle agitator was used as a magnet-driven stirrer. In the procedure, about 700 g of pine oleoresin and 1.4 g of Pd/C catalyst were weighed and placed into the reactor. Then, the reactor was sealed and the air was removed by flushing with nitrogen several times. And the vessel was heated to the desired temperature. Samples during the experiment at specified time intervals were taken via the liquid sampling valve, and sent for gas chromatography analysis. The reaction was carried out at 210 °C, 220 °C, 230 °C, 240 °C, 250 °C and 260 °C, individually.

For a quantitative analysis of the samples involved in the disproportionation reaction scheme, a GC analytical procedure was performed on a Varian CP-3380 GC equipped with a DB-5 column ($L=30$ m, $ID=0.25$ mm and film thickness $=0.25$ μm) and an FI-detector. Injector and detector temperatures were set at 250 °C. The oven temperature was programmed from 55 °C to 80 °C at 1 °C min^{-1} , at 20 °C min^{-1} to 160 °C, then at 2 °C min^{-1} to 250 °C. Nitrogen was employed as carrier gas and the injected volume was 0.2 mm^3 .

Qualitative analysis of the reaction species in the samples was carried out using 6890 GC–MS chromatograph equipped with a mass detector MSD type 5973. The sample constituents were separated with an HP-5MS 30 m \times 0.32 mm \times 0.25 μm column. Helium (99.999% purity) was the carrier gas at a flow rate of 1.0 ml min^{-1} . The MS operating parameters were: ionization voltage of 70 eV; ion source temperature of 250 °C; mass rang of 35–600 amu. Injector and detector temperatures were set at 260 and 270 °C, respectively. The temperature program of the column was set as follows: from 55 to 75 °C with rate of 1 °C min^{-1} , then from 75 to 165 °C with rate of 30 °C min^{-1} , and finally from 165 to 250 °C with rate of 3 °C min^{-1} . Compounds were identified from the program data bank, National Institute of Standards and Technology Database (NIST), and by comparison of the chromatograms with the literatures (Loeblich and Lawrence, 1956; Song and Liang, 1997; Wang et al., 2007a,b).

3. Results and discussion

3.1. The elimination of internal and external mass transfer limitations

Catalytic disproportionation of pine oleoresin over a Pd/C catalyst is a liquid–solid two-phase reaction. The reaction occurs at the liquid–catalyst interface. Therefore, the internal and external mass transfer limitations can influence the reaction (Devulapelli and Weng, 2009). In order to determine the kinetic model in a pure kinetic regime, several preliminary runs were carried out to investigate the effects of internal and external diffusion. It was found that the impacts of external and internal mass transfer limitations on the observed kinetics were negligible.

First, the rotational speed was varied between 150 and 600 rpm to study the external mass transfer resistance. As shown in Fig. 1, the conversion increased with increase of rotational speed from 150 to 400 rpm. However, conversion remained almost constant at rotational speed beyond 400 rpm. Thus, the external diffusion effect was negligible when rotational speed was above 500 rpm. The rotational speed was maintained at 500 rpm for all further experiments.

The absence of intraparticle mass transfer (i.e., internal diffusion) resistance was explored by studying the effect of catalyst particle size (Aki and Abraham, 1999; Cabrera and Grau, 2006). Different runs were carried out in the particle ranges <40 μm to 140–160 μm at 260 °C. As observed in Fig. 2, no differences in conversion rate were found for particle diameters below 60 μm . In this work, the particle size of Pd/C catalyst was between 10 and 20 μm . Hence, the influence of internal mass transfer was negligible.

3.2. Disproportionation reaction scheme and kinetic model

The disproportionation of rosin acids and monoterpenes of pine oleoresin can occur by heat over a Pd/C catalyst (Chen et al.,

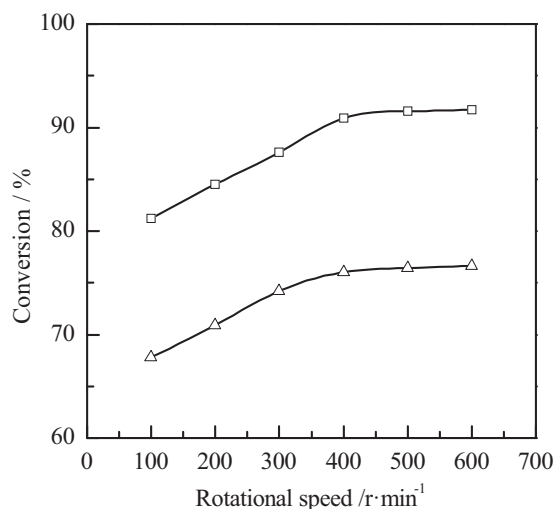


Fig. 1. Effect of stirrer rate on the conversion of rosin acids (□) and bicyclic monoterpenes (Δ) of pine oleoresin. Temperature, 260 °C; reaction time, 15 min; catalyst loading, 0.05% (w/w) of pine oleoresin; pine oleoresin amount, 700 g.

2004; Wang et al., 2007a,b). The disproportionation of oleoresin involves dehydrogenation of rosin acids and bicyclic monoterpenes, as well as hydrogenation and isomerisation reactions, so that the mixture evolves to a final composition that is more stable from a thermodynamical view. The disproportionation of rosin acids in oleoresin has been considered to be an exchange of hydrogen between acid molecules (Song and Liang, 1997; Song et al., 1985; Souto et al., 2011; Wang et al., 2009). The abietic-type resin acids (neoabietic acid, palustric acid and levopimaric acid), via the isomerisation reactions of double bond rearrangement on heating to abietic acid, are stable to heat and acid (Soltes and Zinkel, 1989). Then, abietic acid with conjugated double bonds easily loses its hydrogen atoms and rearranges to form dehydroabietic acid with an aromatic ring. At the same time, other abietic molecules are hydrogenated to become hydrogenated abietic-type resin acids. Meanwhile, pimaric-type acids also accept hydrogen atoms to form hydrogenated pimaric acids. There are multiple isomers of hydrogenated abietic-type resin acids and hydrogenated

pimarenoic-type resin acids in the products (Song and Liang, 1997; Song et al., 1985; Wang et al., 2007b).

The bicyclic monoterpenes of turpentine in pine oleoresin, such as pinene, camphene and carene, are converted to the products monocyclic monoterpenes. The products, such as limonene and terpinene, are obtained by ring-opening isomerization over organic acid proton sources of the rosin acids. Then the monocyclic monoterpenes are transformed into *p*-cymene via dehydroaromatization. On the other hand, the lost hydrogen atoms are absorbed by other monoterpene molecules to form hydrogenation monoterpenes such as carane, camphane and pinane, which is similar to the intermolecular hydrogen transfer of rosin acids (Alsalmeh et al., 2010; Roberge et al., 2001; Wang et al., 2007a).

Pine oleoresin, a biomass resource, as mentioned above, its disproportionation involves dehydrogenation, hydrogenation and isomerisation reactions. And the components of reaction mixtures are complicated. Therefore it is difficult to describe the mixtures kinetics because of a great number of kinetic parameters. Just like the kinetic studies for petroleum processing (Bollas et al., 2007; Hernández-Barajas et al., 2009; Lin et al., 2001; Meng et al., 2006; Singh et al., 2005; Zhou et al., 2008), in order to obtain a simple kinetic model for the disproportionation of oleoresin, similar components are grouped into a few “cuts” or “lumps”. A new complex reaction scheme (see Fig. 3) together with a lumped kinetic model was first proposed in accordance with the above mentioned reaction characteristics and the lumped methodology. In this scheme, the complex mixtures were divided into 7 lumps, based on similar structures as follows: bicyclic monoterpenes (represented by A), palustric acid (represented by B), pimaric-type resin acids (represented by D), hydrogenated monoterpenes (represented by E), monocyclic monoterpenes (represented by F), hydrogenated pimarenoic-type resin acids (represented by H), and hydrogenated abietic-type resin acids (represented by K); other important compounds such as neoabietic acid (represented by C), abietic acid (represented by G), *p*-cymene (represented by I) and dehydroabietic acid (represented by J). In view of the above, the reaction scheme of the lumped model for the catalytic disproportionation of pine oleoresin could be proposed, as illustrated in Fig. 3.

In this case, the reaction rate equation could be written as follows:

$$R = \frac{dc}{dt} = k \times c^{n_i} \quad (1)$$

where $R = \left[\frac{dc_A}{dt}, \frac{dc_B}{dt}, \frac{dc_C}{dt}, \frac{dc_D}{dt}, \frac{dc_E}{dt}, \frac{dc_F}{dt}, \frac{dc_G}{dt}, \frac{dc_H}{dt}, \frac{dc_I}{dt}, \frac{dc_J}{dt}, \frac{dc_K}{dt} \right]^T$, c_A, c_B, \dots, c_K represents the concentrations of the components and t refers to the observation times; $c^{n_i} = \left[c_A^{n_1}, c_B^{n_2}, c_C^{n_2}, c_D^{n_2}, c_E^{n_1}, c_F^{n_1}, c_G^{n_2}, c_H^{n_2}, c_I^{n_1}, c_J^{n_2}, c_K^{n_2} \right]^T$, n_1 represents reaction order for monoterpenes of oleoresin and n_2 is reaction order for rosin acids of oleoresin; k denotes reaction rate constant matrix, expressed by:

$$k = \begin{bmatrix} -k_1 - k_2 & 0 & 0 & 0 & 0 & 0 & 0 & 0 & 0 & 0 & 0 \\ 0 & -k_4 & 0 & 0 & 0 & 0 & 0 & 0 & 0 & 0 & 0 \\ 0 & 0 & -k_5 & 0 & 0 & 0 & 0 & 0 & 0 & 0 & 0 \\ 0 & 0 & 0 & -k_8 & 0 & 0 & 0 & 0 & 0 & 0 & 0 \\ 0 & 0 & 0 & 0 & k_1 & 0 & 0 & 0 & 0 & 0 & 0 \\ 0 & 0 & 0 & 0 & k_2 & -k_3 & 0 & 0 & 0 & 0 & 0 \\ 0 & k_4 & k_5 & 0 & 0 & 0 & -k_6 - k_7 & 0 & 0 & 0 & 0 \\ 0 & 0 & 0 & 0 & 0 & 0 & 0 & k_8 & 0 & 0 & 0 \\ 0 & 0 & 0 & 0 & 0 & 0 & 0 & 0 & k_3 & 0 & 0 \\ 0 & 0 & 0 & 0 & 0 & 0 & 0 & 0 & 0 & k_6 & 0 \\ 0 & 0 & 0 & 0 & 0 & 0 & 0 & 0 & 0 & 0 & k_7 \end{bmatrix} \quad (2)$$

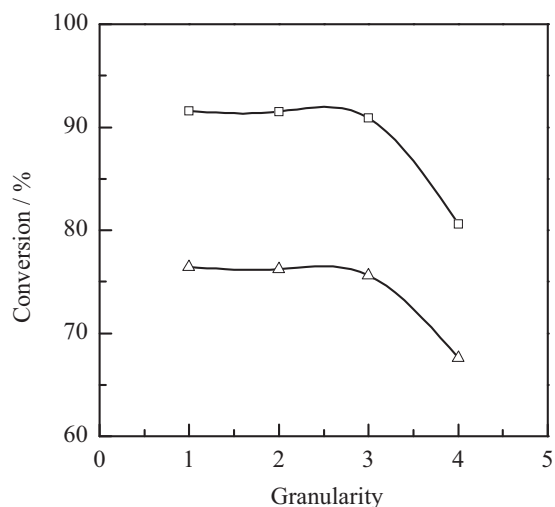


Fig. 2. Variation of the conversion of rosin acids (□) and bicyclic monoterpenes (Δ) of pine oleoresin with granularity of catalyst [granularity of catalyst: 1 (<40 μm); 2 (60–80 μm); 3 (100–120 μm); 4 (140–160 μm)]. Temperature, 260 °C; reaction time, 15 min; stirring rate, 500 rpm; catalyst loading, 0.05% (w/w) of pine oleoresin; pine oleoresin amount, 700 g.

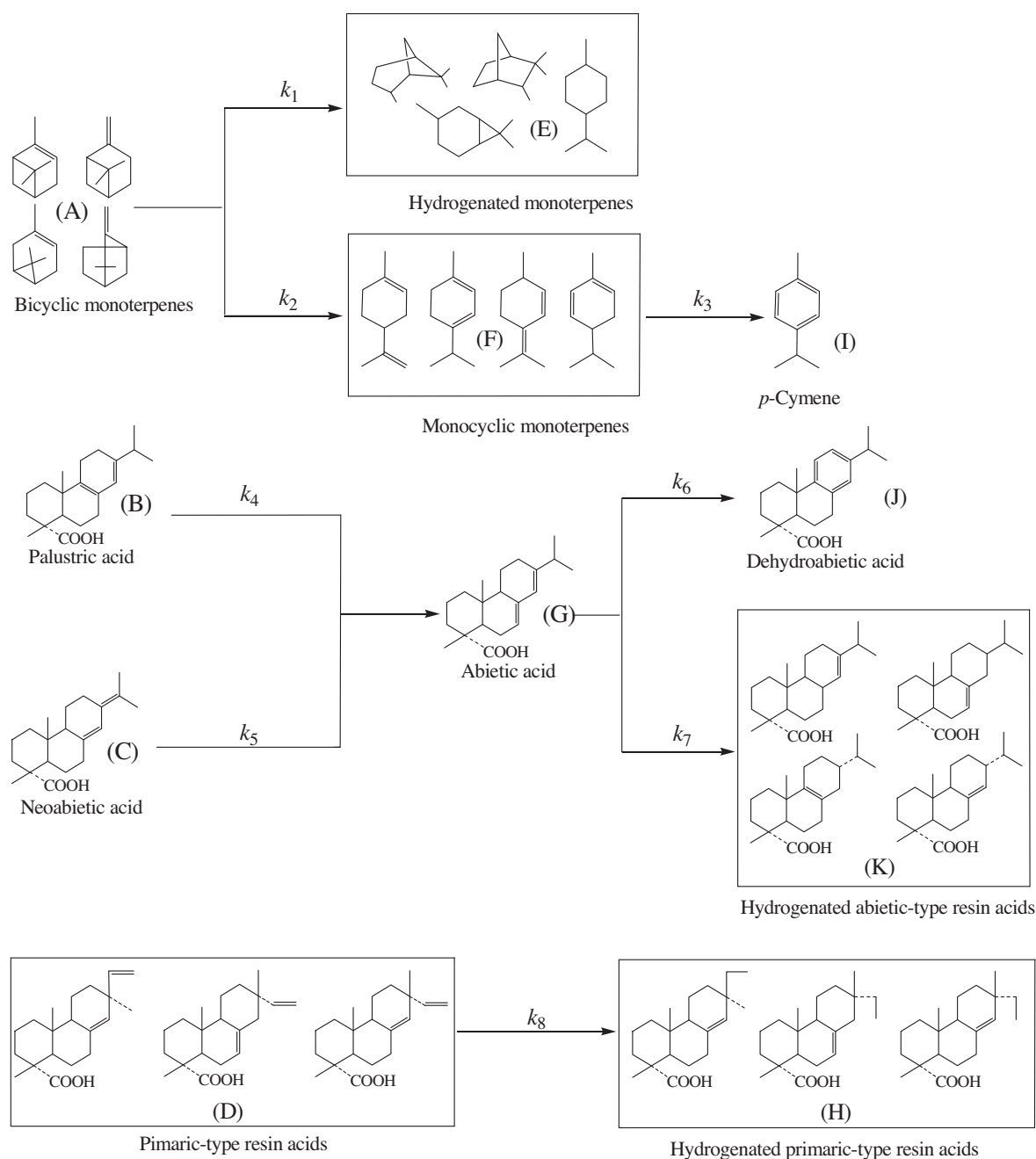


Fig. 3. The reaction scheme for catalytic disproportionation of pine oleoresin.

The mass fraction of each composition was obtained by the quantitative analysis on gas chromatography. And then the mass fraction was converted into mole concentration through the mass balance equation as follows:

$$c_i = 1000(\omega_i \times G \times d)/(M_i \times W) \quad (3)$$

3.3. Modeling results

The rate constants (k) of the kinetic model were estimated using the Levenberg–Marquart nonlinear least-squares method (Marquardt, 1963), using a program written for the optimization in MATLAB (Constantinides and Mostoufi, 1999). The following

objective function (Q) was minimized between calculated and experimental results during the parameter estimation:

$$Q = \sum (c_i(t) - \hat{c}_i(t))^2 \quad (4)$$

The reaction order was determined by try-and-error method, in which n_1 and n_2 were assumed as 0.5, 1.0, 1.5, 2 and 2.5, respectively. The estimated parameters were restricted to be greater than zero in the regression algorithm, as physical sense existed.

The rate constants along with their limits of confidence interval at different temperatures were estimated based on 65 groups of data with the results presented in Table 1. Besides, the reaction orders were obtained, i.e., $n_1 = 1$ and $n_2 = 2$. The experimental results (symbols) of each component compared with the calculated

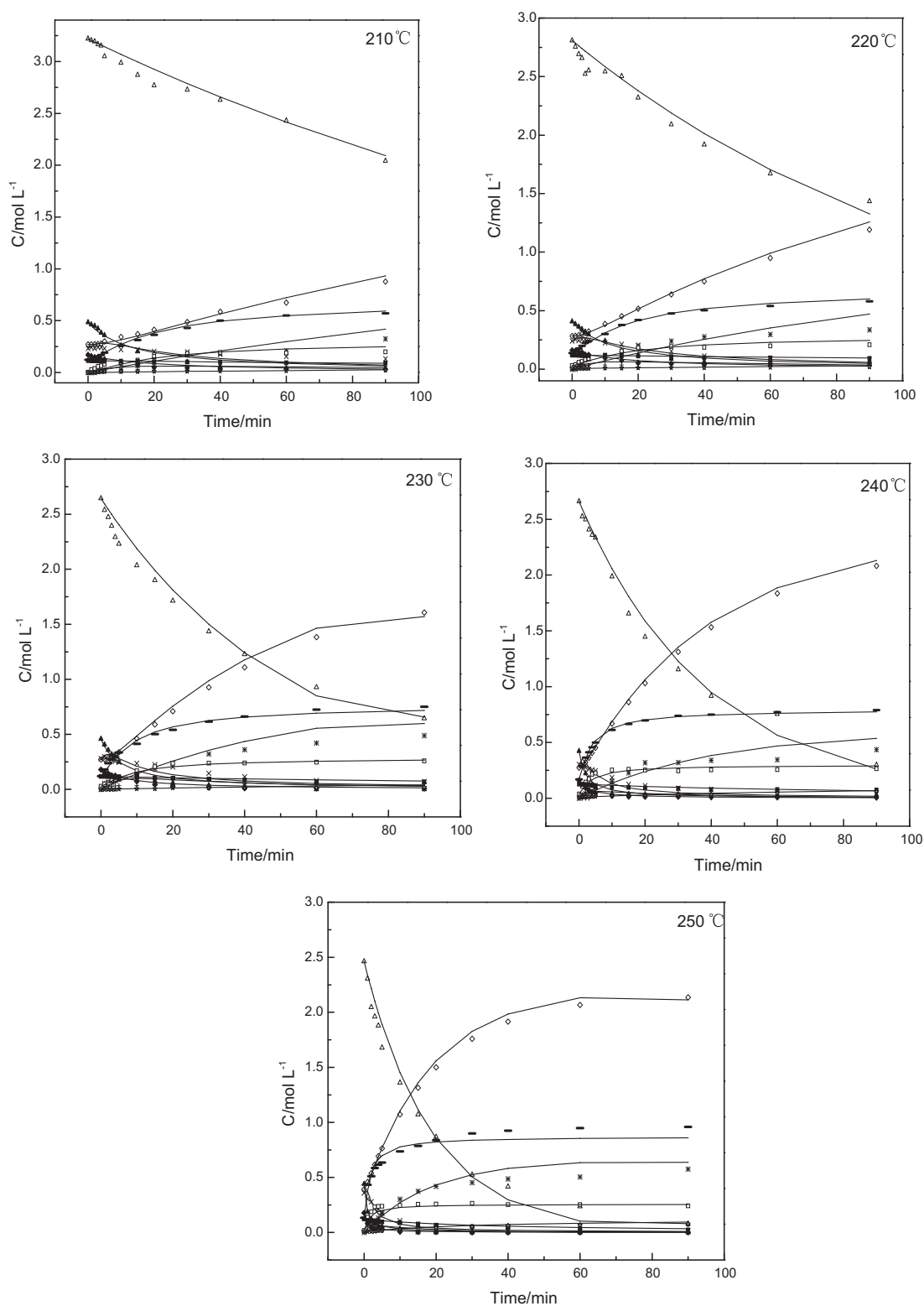


Fig. 4. Comparison between the experimental and computed results of the concentration of components at different temperatures. Solid lines are calculated results and symbols are experimental results for bicyclic monoterpenes (Δ), palustric acid (\blacktriangle), neoabietic acid (\triangle), pimaric-type resin acids (\blacksquare), hydrogenated monoterpenes ($*$), monocyclic monoterpenes ($+$), abietic acid (\times), dehydroabietic acid ($-$), *p*-cymene (\triangle), hydrogenated abietic-type resin acids (\square), hydrogenated pimarenoic acid-type resin acids (\star). Reaction time, 90 min; stirring rate, 500 rpm; catalyst loading, 0.05% (w/w) of pine oleoresin; pine oleoresin 700 g.

Table 1
Parameter estimation results for the model of pine oleoresin disproportionation.

Temperature (°C)	k_1 (min ⁻¹)	k_2 (min ⁻¹)	k_3 (min ⁻¹)	k_4 (L mol ⁻¹ min ⁻¹)
210	0.001777 ± 0.00002561	0.003014 ± 0.0002920	0.1395 ± 0.07835	0.1563 ± 0.02468
220	0.002649 ± 0.0003773	0.005677 ± 0.0004413	0.2028 ± 0.02143	0.2228 ± 0.08363
230	0.005771 ± 0.0006485	0.013022 ± 0.0009730	0.2858 ± 0.07405	0.3735 ± 0.06093
240	0.005870 ± 0.0007950	0.020049 ± 0.0009432	0.7549 ± 0.09668	1.1282 ± 0.1967
250	0.014203 ± 0.001652	0.038628 ± 0.002471	1.277096 ± 0.250962	2.9778 ± 0.5387
Temperature (°C)	k_5 (L mol ⁻¹ min ⁻¹)	k_6 (L mol ⁻¹ min ⁻¹)	k_7 (L mol ⁻¹ min ⁻¹)	k_8 (L mol ⁻¹ min ⁻¹)
210	0.2230 ± 0.08330	0.1608 ± 0.03411	0.1068 ± 0.02104	0.01548 ± 0.002929
220	0.3712 ± 0.09967	0.2626 ± 0.02622	0.1231 ± 0.01468	0.02297 ± 0.004830
230	0.6875 ± 0.1283	0.4298 ± 0.06242	0.1721 ± 0.02955	0.04958 ± 0.01290
240	2.1241 ± 0.8240	0.7939 ± 0.1004	0.3315 ± 0.04696	0.08209 ± 0.01556
250	5.7776 ± 0.9398	1.4616 ± 0.2723	0.4732 ± 0.09665	0.2398 ± 0.04838

results (solid lines) at 210–250 °C are showed in Fig. 4. The activation energy (E_a) and frequency factor (k_0) were calculated with the Arrhenius equation (see Eq. (5)) by linear regress with the rate constants in different temperatures. The high values for the linear correlation coefficient ρ^2 indicated a close match between the experimental and modeled data. The parameter calculation results are summarized in Table 2.

$$k = k_0 \exp(-E_a/RT) \quad (5)$$

3.4. Discussion

The modeling result shows that, under the condition that the diffusion effects have been eliminated, the isomerization and disproportionation of rosin acids appear to be second order reaction while that of monoterpenes first order reaction. This indicates that the concentration of rosin acids has a greater effect on the oleoresin reaction rate than that of monoterpenes.

The parameters in Table 1 reveal that the relationship between the rate constants for the reactions of rosin acids are $k_6 > k_7$. Although dehydroabietic acid with its aryl structure and hydrogenated abietic-type acids with their alicyclic structures are both stable, the rate of abietic acid dehydrogenation (k_6) is higher than that of abietic acid hydrogenation (k_7) during the hydrogen exchange of abietic acid. This is consistent with the fact that dehydroabietic acid forms the main component in the products of rosin acids of disproportionated oleoresin. Likewise, the reaction rate of dehydrogenation of bicyclic monoterpenes is bigger than that of hydrogenation, $k_3 > k_1$, so that *p*-cymene is the main component in the products of monoterpenes of disproportionated oleoresin. Al-Wadaani et al. (2009), Buhl et al. (1998), and Roberge et al. (2001) also reported that the main products for intermolecular hydrogen transfer of pinene and monoterpene mixtures were *p*-cymene on Pd/C catalyst. It means that dehydrogenation is the main reaction in the intermolecular hydrogen transfer reaction (disproportionation) of pine oleoresin over a Pd/C catalyst.

In the unsaturated double bond reactions, it had been observed that rate of the disproportionation of rosin acids was greater than that of monoterpenes. Thus, the formation rates of dehydroabietic

acid and hydrogenated resin acids were greater than that of *p*-cymene and hydrogenation monoterpenes. It can be explained that monoterpenes have isolated unsaturated double bonds, whose formation energy is higher than that of rosin acids with cyclic conjugated double bonds (Buhl et al., 1999). And it can also be explained by the fact that the conjugated species have a higher adsorptivity on catalyst surface (Červený, 1989).

From the data of E_a in Table 2, the activation energies for the hydrogenation of abietic acid and bicyclic monoterpenes are relatively less than those of dehydrogenation. It indicates that the dehydrogenation is more sensitive to reaction temperature than hydrogenation. The selectivity to dehydroabietic acid and *p*-cymene increases among the competing reactions of dehydrogenation and hydrogenation with higher temperatures.

3.5. Verification of the model

The model results were compared with experimental data obtained in the temperature range 210–250 °C. As seen in Fig. 4, the model calculations for the concentrations of each species agreed well with experimental values.

The accuracy of the estimated results from the model was statistically analyzed with the *F*-test at the 95% significance level. It can be seen from Table 1 that all of the estimated parameters in the final optimisation have a reasonable confidence interval, indicating that the experiments for parameter estimation are sufficient. The results of statistic test are shown in Table 3. It is evident that all the correlation coefficients (ρ^2), at various temperatures, are over 0.90, and all of the calculated *F* values are greater than those from *F*_t value (*F*_{0.05}(8, 5)=4.82) multiplied 10, upper quantiles of Fisher's *F* distribution. These results suggest that the kinetic model is significant within the 95% confidence level.

In order to verify the predictive ability of the kinetic model and the reliability of the kinetic parameters, an experiment of oleoresin disproportionation over a Pd/C catalyst was carried out at an extended operation temperature of 260 °C. Fig. 5 presents a comparison between the experimental and computed values at that temperature. It can be observed that the proposed kinetic model performs well for the concentration of each component in the disproportionation of oleoresin at that temperature to determine the model parameters.

Table 2
 E_a and k_0 for each reaction of pine oleoresin disproportionation.

Reaction	E_a (kJ mol ⁻¹)	k_0	ρ^2
A → E	103.97	2.97×10^8 (min ⁻¹)	0.945
A → F	133.82	8.95×10^{11} (min ⁻¹)	0.994
F → I	112.22	1.71×10^{11} (min ⁻¹)	0.953
B → G	159.08	1.77×10^{16} (L mol ⁻¹ min ⁻¹)	0.965
C → G	172.75	8.28×10^{17} (L mol ⁻¹ min ⁻¹)	0.980
G → J	113.96	3.18×10^{11} (L mol ⁻¹ min ⁻¹)	0.991
G → K	83.05	8.68×10^7 (L mol ⁻¹ min ⁻¹)	0.969
D → H	141.65	2.67×10^{13} (L mol ⁻¹ min ⁻¹)	0.981

Table 3
Results of statistical test for the model of pine oleoresin disproportionation.

Temperature (°C)	ρ^2	<i>F</i> _{cal}
210	0.987	170.07
220	0.996	523.95
230	0.991	252.15
240	0.994	402.93
250	0.992	285.96

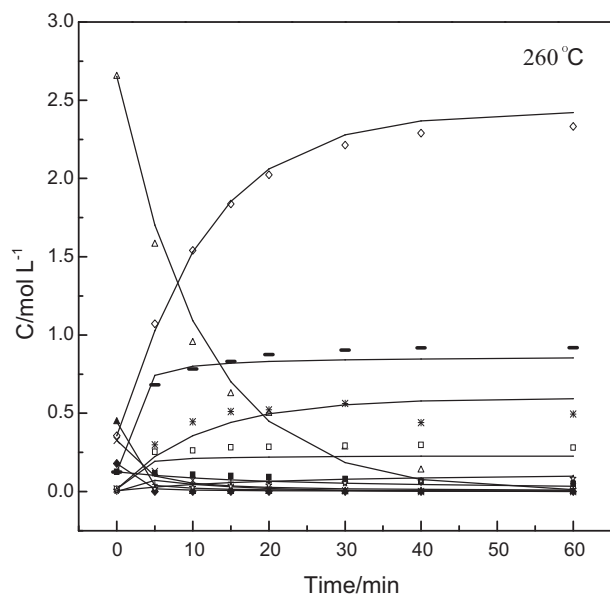


Fig. 5. Comparison between observed and computed values of the concentration of components at 260 °C. Solid lines are calculated value and symbols are experimental value for bicyclic monoterpenes (Δ), palustric acid (\blacktriangle), neoabietic acid (\triangle), pimaric-type resin acids (\blacksquare), hydrogenated monoterpenes (*), monocyclic monoterpenes (+), abietic acid (\times), dehydroabietic acid (—), *p*-cymene (\triangle), hydrogenated abietic-type resin acids (\square), hydrogenated pimaric-type resin acids (Δ). Reaction time, 90 min; stirring rate, 500 rpm; catalyst loading, 0.05% (w/w) of pine oleoresin; pine oleoresin 700g.

4. Conclusions

In this paper, the mass transfer effects of the heterogeneous reaction, the catalytic disproportionation of pine oleoresin over a Pd/C catalyst, were investigated. The external diffusion effect was negligible at rotational speed above 500 rpm. And the internal diffusion was deemed to be absent at sizes of particle diameter below 60 μm . A new reaction scheme and lumped model of Pd/C catalysed disproportionation of oleoresin were proposed according to lumped method. Kinetic experiments in the absence of mass-transport limitation were carried out for 210–260 °C. The kinetic parameters for each involved reaction were estimated using the Levenberg–Marquardt method by MATLAB software. The results revealed that dehydrogenation was the main reaction during intermolecular hydrogen transfer reaction (disproportionation) of oleoresin. The reaction rate of rosin acids was greater than that of monoterpenes. The simulation results found that the model provided a good agreement with the experimental kinetic data and was able to predict the concentration distribution at 260 °C.

Acknowledgements

The authors gratefully acknowledge financial support for this research from the National Natural Science Foundation of China (31060102), the Natural Science Foundation of Guangxi Autonomous Region (2013GXNSFAA019050) and the Dean Project of Guangxi Key Laboratory of Petrochemical Resource Processing and Process Intensification Technology.

References

Aki, S.N.V.K., Abraham, M.A., 1999. Catalytic supercritical water oxidation of pyridine: kinetics and mass transfer. *Chem. Eng. Sci.* 54, 3533–3542.
 Al-Wadaani, F., Kozhevnikova, E.F., Kozhevnikov, I.V., 2009. Zn(II)–Cr(III) mixed oxide as efficient bifunctional catalyst for dehydroisomerisation of α -pinene to *p*-cymene. *Appl. Catal. A* 363, 153–156.

Alsalmeh, A., Kozhevnikova, E.F., Kozhevnikov, I.V., 2010. α -Pinene isomerisation over heteropoly acid catalysts in the gas-phase. *Appl. Catal. A* 390, 219–224.
 Bollas, G.M., Lappas, A.A., Iatridis, D.K., Vasalos, I.A., 2007. Five-lump kinetic model with selective catalyst deactivation for the prediction of the product selectivity in the fluid catalytic cracking process. *Catal. Today* 127, 31–43.
 Buhl, D., Roberge, D.M., Hölderich, W.F., 1999. Production of *p*-cymene from α -limonene over silica supported Pd catalysts. *Appl. Catal. A* 188, 287–299.
 Buhl, D., Weyrich, P.A., Sachtler, W.M.H., Hölderich, W.F., 1998. Support effects in the Pd catalyzed dehydrogenation of terpene mixtures to *p*-cymene. *Appl. Catal. A* 171, 1–11.
 Cabrera, M.I., Grau, R.J., 2006. Liquid-phase hydrogenation of methyl oleate on a Ni/ α - Al_2O_3 catalyst: a study based on kinetic models describing extreme and intermediate adsorption regimes. *J. Mol. Catal. A: Chem.* 260, 269–279.
 Červený, L., 1989. Palladium catalysts in hydrogenation reactions. *Chem. Eng. Commun.* 83, 31–63.
 Chen, X.P., Wang, L.L., Zhu, Y.J., 2004. China Patent No. 2004100783722.
 Constantinides, A., Mostoufi, N., 1999. Numerical Methods for Chemical Engineers with MATLAB Applications. Prentice Hall, New Jersey.
 Devulapelli, V.G., Weng, H.-S., 2009. Synthesis of cinnamyl acetate by solid-liquid phase transfer catalysis: kinetic study with a batch reactor. *Catal. Commun.* 10, 1638–1642.
 Drelinkiewicz, A., Waksmundzka-Góra, A., 2006. Investigation of 2-ethylanthraquinone degradation on palladium catalysts. *J. Mol. Catal. A: Chem.* 246, 167–175.
 Enos, H.I., Harris, G.C., Hedrick, G.W., 1968. Rosin and Rosin Derivatives, second ed. Wiley, New York, pp. 475–508.
 Gu, W., Wang, S.F., 2010. Synthesis and antimicrobial activities of novel 1H-dibenzo[a,c]carbazoles from dehydroabietic acid. *Eur. J. Med. Chem.* 45, 4692–4696.
 Häkkinen, S.T., Lackman, P., Nygrén, H., Oksman-Caldentey, K.-M., Maaheimo, H., Rischer, H., 2012. Differential patterns of dehydroabietic acid biotransformation by *Nicotiana tabacum* and *Catharanthus roseus* cells. *J. Biotechnol.* 157, 287–294.
 Hernández-Barajas, J.R., Vázquez-Román, R., Félix-Flores, M.G., 2009. A comprehensive estimation of kinetic parameters in lumped catalytic cracking reaction models. *Fuel* 88, 169–178.
 Lin, Y.H., Hwu, W.H., Ger, M.D., Yeh, T.F., Dwyer, J., 2001. A combined kinetic and mechanistic modelling of the catalytic degradation of polymers. *J. Mol. Catal. A: Chem.* 171, 143–151.
 Loeblich, V., Lawrence, R., 1956. Chromatographic investigation of disproportionated rosin. *J. Am. Oil Chem. Soc.* 33, 320–322.
 Marquardt, D.W., 1963. An algorithm for least-squares estimation of nonlinear parameters. *J. Soc. Ind. Appl. Math.* 11, 431–441.
 Martín-Luengo, M.A., Yates, M., Martínez Domingo, M.J., Casal, B., Iglesias, M., Esteban, M., Ruiz-Hitzky, E., 2008. Synthesis of *p*-cymene from limonene: a renewable feedstock. *Appl. Catal. B* 81, 218–224.
 Martín-Luengo, M.A., Yates, M., Rojo, E.S., Huerta Arribas, D., Aguilar, D., Ruiz Hitzky, E., 2010. Sustainable *p*-cymene and hydrogen from limonene. *Appl. Catal. A* 387, 141–146.
 Mayer, M.J.J., Meuldijk, J., Thoenes, D., 1996. Emulsion polymerization of styrene with disproportionated rosin acid soap as emulsifier. *J. Appl. Polym. Sci.* 59, 1047.
 Meng, X.H., Xu, C.M., Gao, J.S., Li, L., 2006. Catalytic pyrolysis of heavy oils: 8-lump kinetic model. *Appl. Catal. A* 301, 32–38.
 Piang-Siong, W., de Caro, P., Lacaze-Dufaur, C., Shum Cheong Sing, A., Hoareau, W., 2012. Effect of catalytic conditions on the synthesis of new aconitate esters. *Ind. Crops Prod.* 35, 203–210.
 Rajakumar, P., Sekar, K., Shanmugaiyah, V., Mathivanan, N., 2009. Synthesis of novel carbazole based macrocyclic amides as potential antimicrobial agents. *Eur. J. Med. Chem.* 44, 3040–3045.
 Rezzi, S., Bighelli, A., Castola, V., Casanova, J., 2005. Composition and chemical variability of the oleoresin of *Pinus nigra* ssp. *laricio* from Corsica. *Ind. Crops Prod.* 21, 71–79.
 Roberge, D.M., Buhl, D., Niederer, J.P.M., Hölderich, W.F., 2001. Catalytic aspects in the transformation of pinenes to *p*-cymene. *Appl. Catal. A* 215, 111–124.
 Singh, J., Kumar, M.M., Saxena, A.K., Kumar, S., 2005. Reaction pathways and product yields in mild thermal cracking of vacuum residues: a multi-lump kinetic model. *Chem. Eng. J.* 108, 239–248.
 Soltes, E.J., Zinkel, D.F., 1989. Chemistry of Rosin. Pulp Chemicals Association, New York, pp. 261–345.
 Song, Z.Q., 2004. Researches on pine chemicals in china. *Chem. Ind. Forest Prod.* 24, 7–11.
 Song, Z.Q., Liang, Z.Q., 1997. Study on reaction mechanism of disproportionation of Chinese gum rosin catalysed by palladium-on-charcoal. *Chem. Ind. Forest Prod.* 17, 13–17.
 Song, Z.Q., Zavarin, E., Zinkel, D.F., 1985. On the palladium-on-charcoal disproportionation of rosin. *J. Wood Chem. Technol.* 5, 535–542.
 Song, Z.Q., Liang, Z.Q., Liu, X., 1995. Chemical characteristics of oleoresins from Chinese pine species. *Biochem. Syst. Ecol.* 23, 517–522.
 Souto, J.C., Yustos, P., Ladero, M., García-Ochoa, F., 2011. Disproportionation of rosin on an industrial Pd/C catalyst: reaction pathway and kinetic model discrimination. *Bioresour. Technol.* 102, 3504–3511.
 Thevissen, K., Marchand, A., Chaltin, P., Meert, E.M.K., Cammue, B., 2009. Antifungal carbazoles. *Curr. Med. Chem.* 16, 2205–2211.
 Tike, M.A., Mahajani, V.V., 2006. Studies in catalytic transfer hydrogenation of soybean oil using ammonium formate as donor over 5% Pd/C catalyst. *Chem. Eng. J.* 123, 31–41.

- Wang, L.L., Sun, W.J., Chen, X.P., Hu, X.G., Fa, T.Z., 2007a. Study on catalytic disproportionation of pine gum over Pd/C. *J. Chem. Eng. Chin. Univ.* 21, 784–789.
- Wang, L.L., Xu, X., Chen, X.P., Sun, W.J., Tong, Z.F., 2007b. Characterization of the reaction products from pine gum catalytic disproportionation by gas chromatography/mass spectrometry. *Chin. J. Chromatogr.* 25, 413–417.
- Wang, L.L., Chen, X.P., Liang, J.Z., Chen, Y.Y., Pu, X.D., Tong, Z.F., 2009. Kinetics of the catalytic isomerization and disproportionation of rosin over carbon-supported palladium. *Chem. Eng. J.* 152, 242–250.
- Wang, Y.C., Su, C.H., Li, F.Y., Liu, L.Z., Pan, Y.M., Wu, X.R., Wang, H.S., 2010. Syntheses, characterization and fluorescent properties of two series of dehydroabietic acid C-ring derivatives. *Spectrochim. Acta A* 76, 328–335.
- Zhang, Q.G., Bi, L.W., Zhao, Z.D., Chen, Y.P., Li, D.M., Gu, Y., Wang, J., Chen, Y.X., Bo, C.Y., Liu, X.Z., 2010. Application of ultrasonic spraying in preparation of p-cymene by industrial dipentene dehydrogenation. *Chem. Eng. J.* 159, 190–194.
- Zhou, H.Q., Wang, Y., Wei, F., Wang, D.Z., Wang, Z.W., 2008. Kinetics of the reactions of the light alkenes over SAPO-34. *Appl. Catal. A* 348, 135–141.